1st International Conference on Sensing Technology
November 21-23, 2005 Palmerston North, New Zealand

A New Micro–Meter Displacement Sensor

T S Rathore, U P Khot
Department of Electrical Engineering,
IIT Bombay, Powai, Mumbai 400 076, India
tsrathor@ee.iitb.ac.in

Abstract

A high-frequency oscillator based capacitive displacement sensor is proposed. It can measure very small displacements of the order of few microns with high sensitivity. Out of the two alternatives which yield an independent control of condition of oscillation and the frequency of oscillation, capacitor-tuned one is more practicable to the resistor-tuned one. The sensor is initially designed and simulated for measurement of ± 5 μm. It is found that the simulated displacements are always less than the expected ones in a proportionate magnitude perhaps due to the non-idealities of the active device used. The sensor works very closely linearly when the displacements lie in the range of $\pm$(2 to 5) μm. The non-ideality error is compensated suitably and the displacement is offset by -3.5 μm so that the sensor operates accurately in the range ± 1.5 μm. The displacement is positive (negative) if the output frequency is larger (smaller) than that without any displacement. This will require less complex circuitry for displaying the direction of the displacement as compared to the case of an LVDT. The sensor is compared with the two alternative sensors: one derived using $RC : CR$ transformation on the above sensor and the other based on the twin-T oscillator.

Keywords: Differential capacitive sensors, oscillators

1 Introduction

Differential capacitive sensors are used to detect the changes of several physical variables like force, position, angular speed, liquid level, pressure, fluidic flow, etc. [1]. Recently, Pennisi has proposed a current-mode differential-capacitance transducer which converts capacitance to current [2]. Though this transducer provides linear relation between the displacement and the output current, it requires a constant current source.

A new high-frequency oscillator based sensor circuit, which can have independent control of condition of oscillation and frequency of oscillation if suitable variables are chosen, is proposed. The oscillator when used as a capacitive displacement sensor, its frequency varies with high linearity with the displacement over a range with a high sensitivity. The sensor is suitable for measurement of very small displacements without any elaborate circuitry for displaying the direction of displacement as in the case of LVDT. The proposed sensor circuit with two alternatives which can yield an independent control of condition of oscillation and the frequency of oscillation is introduced in section 2. Section 3 develops a systematic design of the proposed sensor circuit. The simulated results and the comparison with the other sensors are given in section 4 and 5, respectively.

2 Proposed oscillator based sensor circuit

The proposed bridged-ladder oscillator (BLO) based sensor circuit is shown in figure 1 where operational transresistance amplifier (OTRA) has the terminal characteristics [3]:

$$\begin{bmatrix} V_p \\ V_n \\ V_z \end{bmatrix} = \begin{bmatrix} 0 & 0 & 0 \\ 0 & 0 & 0 \\ R_m & -R_m & 0 \end{bmatrix} \begin{bmatrix} I_p \\ I_n \\ I_z \end{bmatrix}. \quad (1)$$

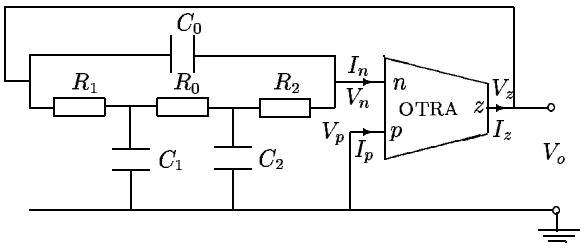

Figure 1: BLO based sensor circuit.

Assuming ideal OTRA ($R_m = \infty$), application of Barkhausen's criterion [4] leads to the condition for sinusoidal oscillation (CO) as

$$\frac{1}{C_0} = (R_0 + R_1 + R_2) \times \left[\frac{1}{C_1 R_1} + \frac{1}{C_2 R_2} + \frac{1}{R_0}\left(\frac{1}{C_1} + \frac{1}{C_2}\right)\right] \quad (2)$$

and the frequency of oscillation (FO)

$$\omega_0 = \sqrt{\frac{1}{C_1C_2}\left[\frac{1}{R_1R_2} + \frac{1}{R_0}\left(\frac{1}{R_1} + \frac{1}{R_2}\right)\right]}. \quad (3)$$

Choosing $R_1 = R_2 = R$ and $R_0 = kR$, from equations (2) and (3) we get

$$\text{CO:} \quad \frac{1}{C_0} = \frac{(1+k)(2+k)}{k}\left(\frac{1}{C_1} + \frac{1}{C_2}\right) \quad (4)$$

and

$$\text{FO:} \quad \omega_0 = \frac{1}{R}\sqrt{\frac{1}{C_1C_2}\left(\frac{2+k}{k}\right)}. \quad (5)$$

Though CO can be satisfied by adjusting C_0, FO cannot be adjusted independently. To achieve independent adjustment of both CO and FO, we have two alternatives.

2.1 Capacitor-tuned oscillator

In equations (4) and (5), adjusting C_1, C_2 keeping $(\frac{1}{C_1} + \frac{1}{C_2})$ constant, FO can be tuned without disturbing the CO and C_0 can be adjusted to satisfy the CO without affecting FO. However, it is practically inconvenient to change C_1 and C_2 keeping $\left(\frac{1}{C_1} + \frac{1}{C_2}\right)$ constant. But, if C_1 and C_2 represent the push-pull arrangement as shown in figure 2 such that $C_{1,2} = \frac{\epsilon A}{d_{1,2}}$ where ϵ is the dielectric constant, A $(= b \times 2l)$ is the area of the capacitor plate, $2l$ is the length and b is the breadth of the plates, $2d$ is the total distance between the fixed plates, $d_1 = d + x$ and $d_2 = d - x$, x is the displacement, then

$$\text{CO:} \quad \frac{1}{C_0} = \frac{(1+k)(2+k)}{\epsilon 2lbk}(2d) \quad (6)$$

and

$$\text{FO:} \quad \omega_0 = \frac{1}{\epsilon 2lbR}\sqrt{(d^2 - x^2)\left(\frac{2+k}{k}\right)}. \quad (7)$$

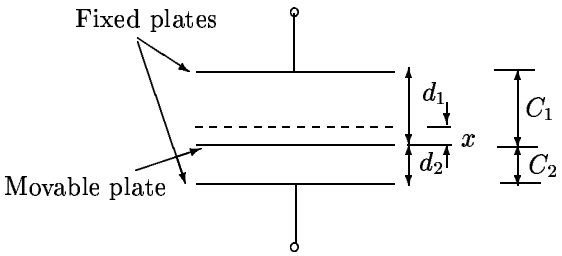

Figure 2: Push-pull type variable displacement capacitor.

CO and FO can now be adjusted independently if C_0 and x are chosen as the variables.

2.2 Resistor-tuned oscillator

Let $C_1 = C_2 = C$. Then from equations (4) and (5) we get

$$\text{CO:} \quad \frac{C_0}{C} = \frac{1}{2}\left[\frac{k}{(1+k)(2+k)}\right], \quad (8)$$

and

$$\text{FO:} \quad \omega_0 = \frac{1}{CR}\sqrt{\frac{2+k}{k}}. \quad (9)$$

Case (i): Choosing $k = 1$ so as to have equal-valued resistors, we get

$$\text{CO:} \quad C_0 = 0.0833C \quad (10)$$

and corresponding

$$\text{FO:} \quad \omega_0 = \frac{\sqrt{3}}{RC}. \quad (11)$$

Thus, CO and FO both can be adjusted independently by varying C_0 and R, respectively. However, a three ganged resistor arrangement is required for this purpose.

Case (ii): The plot of C_0/C vs k as given by equation (8) is shown in figure 3. Note that C_0 is always less than C for any value of k. Therefore, the three capacitors cannot be of equal value.

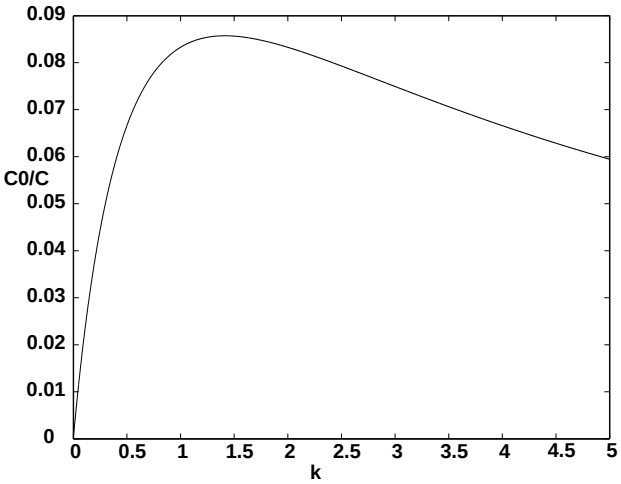

Figure 3: Plot of C_0/C versus k.

However, C_o is closest to C when $k = \sqrt{2}$ and the corresponding C_0 and ω_0 are,

$$C_0 = 0.0858C, \quad (12)$$

$$\omega_0 = \left(\frac{1.5537}{CR}\right). \quad (13)$$

However, this case will not give independent control of CO and FO. Moreover, the value of C_0 is not significantly different from that when $k = 1$. Hence the capacitor-tuned oscillator is preferable

from the practical point of view.

3 Displacement sensor and its design

Equation (7) shows that ω_0 is a function of x. Hence, the oscillator circuit shown in figure 1 can be used as a displacement sensor when the capacitors C_1 and C_2 are arranged as shown in figure 2. The circuit can be designed for specified maximum value of $x = x_m$ and the desired maximum and minimum values of ω_0 at $x = 0$ and $x = x_m$, respectively. As mentioned above, we choose $k = 1$. Then from equation (7) we get

$$\omega_0|_{x=0} = \frac{1}{\epsilon AR} d\sqrt{3} \tag{14}$$

and

$$\omega_0|_{x=x_m} = \frac{1}{\epsilon AR}\sqrt{3(d^2 - x_m^2)} \tag{15}$$

From equations (14) and (15) we get

$$d = \sqrt{\left(\frac{n^2}{n^2-1}\right)} x_m$$

where

$$n = \frac{\omega_0|_{x=0}}{\omega_0|_{x=x_m}}.$$

Now R can be calculated from equation (14). From equation (7)

$$\omega_0 = \frac{d\sqrt{3}}{\epsilon AR}\sqrt{1 - \left(\frac{x}{d}\right)^2}. \tag{16}$$

Therefore,

$$\omega_n = \frac{\omega_0}{\omega_0|_{x=0}} = \sqrt{1-(x_n)^2}, \quad x_n = \frac{x}{d}$$
$$\cong 1 - \frac{1}{2}x_n^2, \quad \text{if } x_n << 1. \tag{17}$$

The plot of normalized frequency ω_n versus x_n is shown in figure 4.

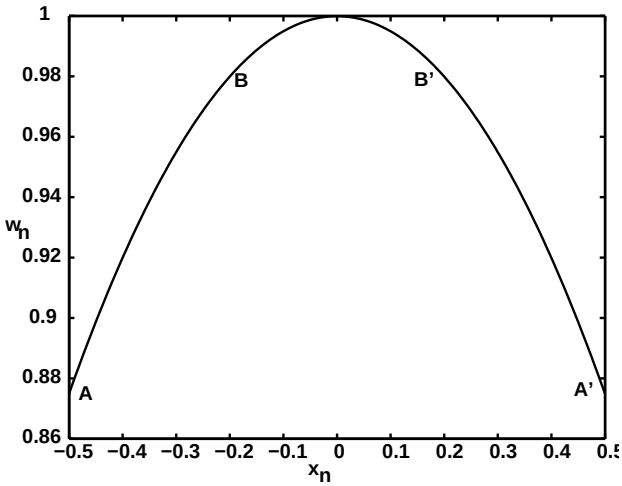

Figure 4: Plot of normalized ω_n versus normalized x_n.

It can be seen that ω_n varies approximately linear in the range AB, A'B'. Hence, the sensor should be operated in these ranges.

The sensor circuit is initially designed for $x_m = \pm 5\ \mu m$, $d = 10\ \mu$m. Choosing the frequency corresponding to x at the middle point of AB (x=$-3.5\ \mu$m) $\omega_0|_{x=-3.5\ \mu m} = 10$ Mrad/sec, air as the dielectric media ($\epsilon = 8.854 \times 10^{-12}$ F/m), $A = 25 \times 25$ mm^2, $k = 1$, R obtained is 293.2 Ω. The corresponding C and C_0 are 0.5534 nF and 0.0461 nF, respectively. The theoretical plot of ω_0 versus x for the designed sensor is shown in figure 5.

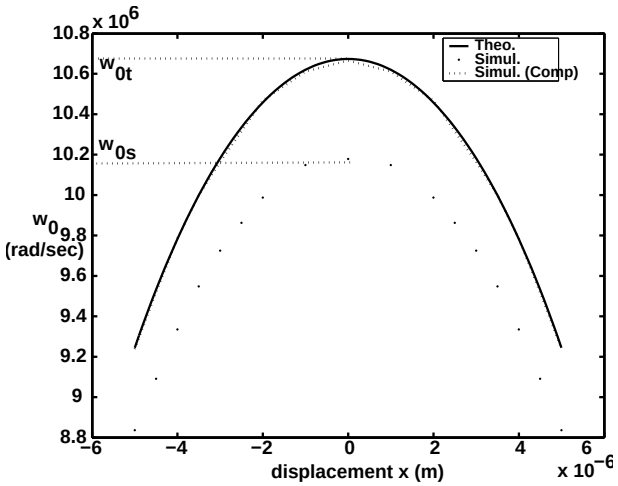

Figure 5: Plot of frequency of oscillation (ω_0) versus displacement (x).

Since the linear region is confined to AB, the displacement is offset by $-3.5\ \mu$m so that $x = 0$ is shifted to C in figure 6. The circuit is therefore suitable for measurement in the range x= $\pm$ 1.5 μm. The displacement is positive (negative) for ω_0 greater (smaller) than 10 Mrad/sec. This fact can be used for displaying the direction of displacement x without elaborate circuitry. The straight line

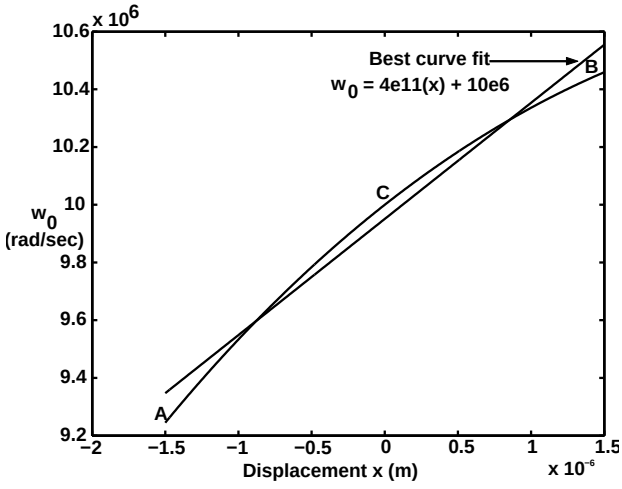

Figure 6: Plot of ω_0 versus x with displacement offset.

(best curve fit) is drawn using the method of least squares from the obtained simulated data and is shown in figure 6. The linearity is simply a measure of maximum deviation of the simulated point from this straight line.

4 Simulated results

The designed sensor circuit is simulated using ORCAD PSPICE. OTRA is realized using commercially available CFAs, AD844s [5]. The displacement x is simulated using various pairs of capacitors (C_1, C_2) such that $\left(\frac{1}{C_1} + \frac{1}{C_2}\right)$ is constant. The simulated plot of x versus ω_0 is also shown in figure 5. The simulated values lie below the theoretical values. This may be due to the non-idealities of OTRA. The error has been componensated by reducing R by a factor $\left(\frac{\omega_{0s}}{\omega_{0t}}\right)$. The frequency variation after the compensation is also shown in figure 5. It can be seen that the plot almost overrides the actual curve.

The $R-$tuned oscillator circuit is also simulated. The theoretical and simulated plots of ω_0 versus R are shown in figure 7.

In both the tunings, once the CO is satisfied, oscillations seen are perfect sine waves over the entire range of x or R without any further tuning, i.e., the change in C_0.

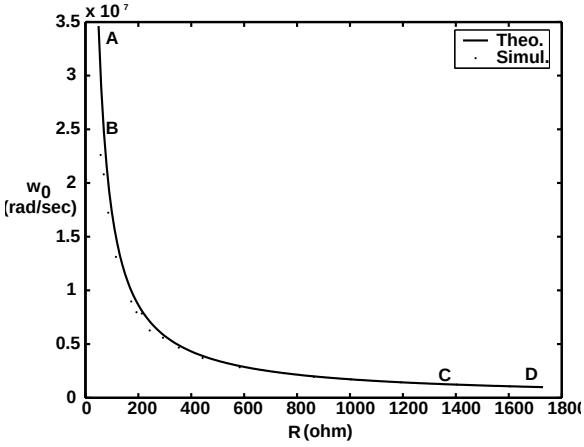

Figure 7: Plot of ω_0 versus R.

5 Comparison with the other sensors

For comparison purpose, we analyze two other ($3C$, $3R$) sensors: one derived from the above sensor using $RC : CR$ transformation and the other based on twin-T oscillator (TTO).

The $RC : CR$ transformation on the circuit of figure 1 gives a sensor circuit shown in figure 8.

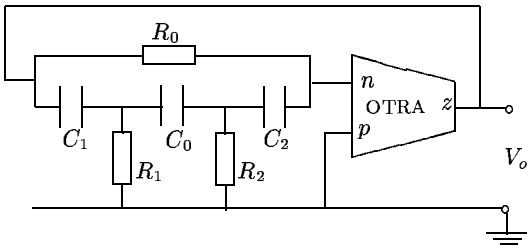

Figure 8: $RC : CR$ Transformed sensor circuit.

Choosing $C_1 = C_2 = C_0 = C$, analysis yields

$$\text{CO}: \quad R_0 = 6(R_1 + R_2) \tag{18}$$

and

$$\text{FO}: \quad \omega_0 = \frac{1}{C}\sqrt{\frac{1}{3R_1R_2}}. \tag{19}$$

Thus, adjusting R_1, R_2 keeping $(R_1 + R_2)$ constant both FO and CO can be adjusted independently. To achieve this, one possible arrangement is shown in figure 9 where $R_{1,2} = \frac{\rho\, l_{1,2}}{A}$, ρ is the resistivity of the material used, A is the cross-sectional area of the resistor, l is the length, $l_1 = l + x$ and $l_2 = l - x$, x is the displacement, then

$$\text{CO}: \quad R_0 = 6\frac{\rho}{A}(l_1 + l_2) \tag{20}$$

and

$$\text{FO}: \quad \omega_0 = \frac{A}{\rho\, C}\sqrt{\frac{1}{3(l^2 - x^2)}}. \tag{21}$$

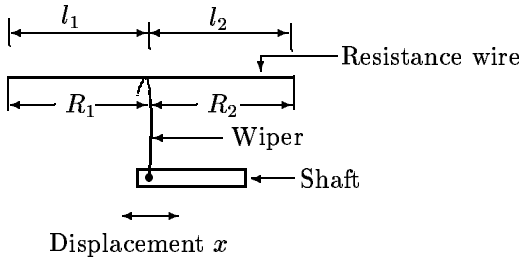

Figure 9: Resistor arrangement.

CO and FO can now be adjusted independently if R_0 and x are chosen as the variables. Thus, it can also be used as a resistive displacement sensor. However, the friction between the wiper and the resistance track results in resolution limitation and less life expectancy [6]. Hence, the original capacitive displacement sensor should be preferred.

Consider another sensor based on twin-T oscillator shown in figure 10.

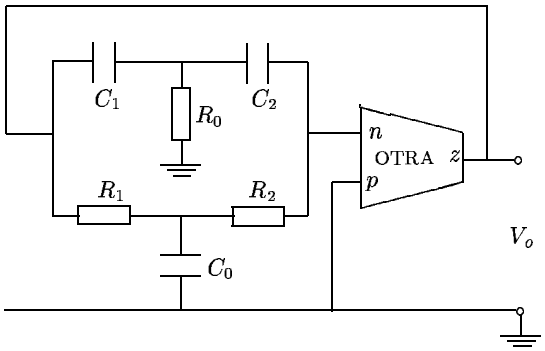

Figure 10: TTO based sensor circuit.

Choosing $R_1 = R_2 = R_0 = R$, analysis gives

$$\text{CO}: \quad \frac{1}{C_0} = \frac{1}{2(C_1 + C_2)} \tag{22}$$

and

$$\text{FO}: \quad \omega_0 = \frac{1}{R}\sqrt{\frac{1}{2C_1C_2}}. \tag{23}$$

Thus, adjusting C_1, C_2 keeping $(C_1 + C_2)$ constant, both FO and CO can be adjusted independently. To adopt the oscillator as a displacement sensor, let C_1 and C_2 be arranged as shown in figure 11 where $C_{1,2} = \frac{\epsilon A_{1,2}}{d}$, ϵ is the dielectric constant, d is the distance between the fixed and movable plates, $A_{1,2} = l_{1,2} \times b$, $l_1 = l + x$, $l_2 = l - x$ where $2l$ is the length and b is the bredth of the plates, x is the displacement and $x < l$, then

$$\text{CO}: \quad \frac{1}{C_0} = \frac{d}{2\epsilon b}\left(\frac{1}{2l}\right) \tag{24}$$

and

$$\text{FO}: \quad \omega_0 = \frac{d}{\epsilon R b}\sqrt{\frac{1}{2(l^2 - x^2)}}. \tag{25}$$

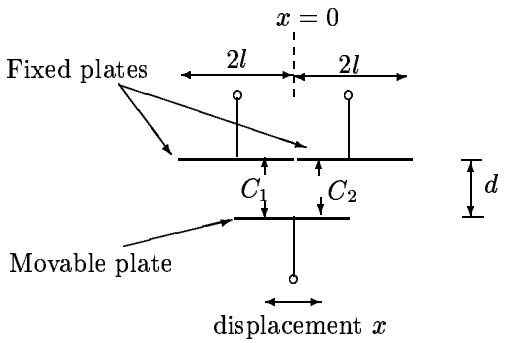

Figure 11: Capacitor arrangement in TTO based displacement sensor.

Thus, CO and FO can be adjusted independently if C_0 and x are chosen as the variables. Thus, it can also be used as a capacitive displacement sensor.

This sensor is designed with the following specifications: $x_m = \pm$ 1.5 mm, $d = 10$ μm, $\omega_0|_{x=0} = 10$ Mrad/sec, air as the dielectric media, $l_1 = l_2 = 25$ mm, $b = 25$ mm, R=127.78 Ω, C=0.553 nF and C_0= 2.212 nF. The theoretical plot of ω_0 versus x after the displacement offset is shown in figure 12. Note that, in both the equations (21) and (25), the term $(l^2 - x^2)$ appears in the denominator. Hence the nature of the plot of ω_0 versus x in both the cases will be the same.

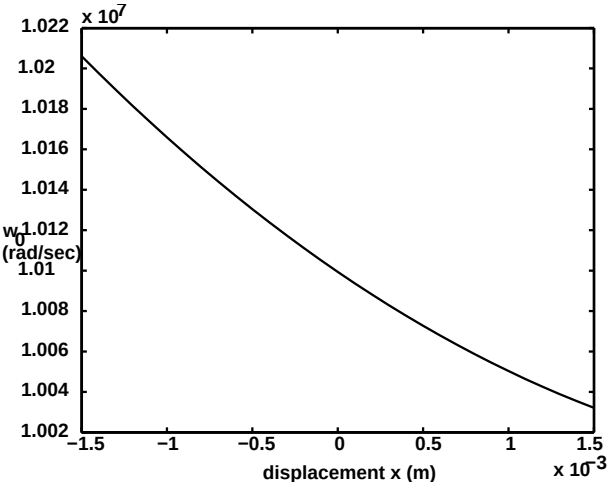

Figure 12: Plot of ω_0 versus x with displacement offset.

Table 1 gives a comparison of the total capacitance C_t required by the two capacitive sensors based on BLO and TTO for the same ω_0 $(=\frac{1}{\sqrt{6}RC})$, and the same total resistance R_t (=3R). BLO based displacement sensor requires less total capacitance C_t. This will lead to less space and high speed of operation in integrated circuits [7].

Table 1: Comparison of total capacitance C_t and various quality parameters.

Displacement sensor circuit →	BLO based	TTO based
C_t	8.84 C	10.39 C
Sensitivity (Hz/m)	4×10^{11}	5.8×10^6
Span	-1.5 to $+1.5$ μm	-1.5 to $+1.5$ mm
Resolution	15 nm	1 mm
Non-linearity % of F. S.	8.419	6.896

Table 1 also shows the sensitivity, span, resolution, non-linearity observed for the same ω_0 =10 Mrad/sec at x=0. It can be seen that the BLO based displacement sensor is superior to the TTO one as the former sensor can measure smaller displacements with better resolution and improved

linearity. The BLO based displacement sensor measures the displacement in the direction perpendicular to length of the plate whereas the TTO based displacement sensor measures it along the length of the plate.

6 Conclusion

A new high frequency oscillator based micro-meter displacement sensor has been proposed. Though both C-tuned and R-tuned oscillators give independent control of CO and FO, the former is more practicable and ideally suited for the displacement sensor. The sensor can measure small displacements of the order of few microns accurately with large sensitivity and better linearity. The effect of non-idealities of the OTRA has been compensated. An offset in the displacement has been introduced so that the sensor operates in the linear region for its entire range. This also simplifies the circuitry required for displaying the direction of the displacement. The BLO based displacement sensor has been compared with two alternatives: one derived using $RC : CR$ transformation on it and the other based on TTO. It has been found that it can measure extremely small displacements with better resolution and linearity. Moreover, it requires less total capacitance and hence should be preferred for integration. The simulated results are found in close agreement with the theoretical ones.

7 References

[1] Baxter, L. K., *Capacitive Sensors Design and Applications*, IEEE Press, New York (1997).

[2] Pennisi, S., "High-performance and simple CMOS interface circuit for differential capacitive sensors", *IEEE Trans. Circuits Syst. II*, vol 52, no 6, pp 327-330 (2005).

[3] Cakir, C., Cam, U., and Cicekoglu, O., "Novel allpass filter configuration employing single OTRA", *IEEE Trans. Circuits Syst. II*, vol 52, no 3, pp 122-125 (2005)

[4] Milliman, J., *Microelectronics Digital and Analog Circuits and Systems*, McGraw-Hill International Book Comp. Ltd. (1983).

[5] Svoboda, J. A., Megary, L., and Webb, S., "Application of a commercially available current conveyor", *Int. J. Electron.*, vol 70, pp 159-164 (1991).

[6] Morris, A. S., *Principles of Measurement and Instrumentation* Prentice-Hall International (UK) Ltd. (1990).

[7] Moore, G. E., "Cramming more components onto integrated circuits", *IEEE Proc.*, vol 86, no 1, pp 82-85 (1998).